Drug Delivery and Translational Research (2021) 11:1943–1957
https://doi.org/10.1007/s13346-020-00856-8

ORIGINAL ARTICLE

Promising bioadhesive ofloxacin-loaded polymeric nanoparticles for the treatment of ocular inflammation: formulation and in vivo evaluation

Alaa H. Salama[1,2] · Mona M. AbouSamra[1] · Ghada E. A. Awad[3] · Soheir S. Mansy[4]

Accepted: 9 September 2020 / Published online: 2 October 2020

Abstract

Our work tackles the combined advantages of both nanotechnology and the bioadhesive gel properties which were utilized to design an ocular drug delivery system that is capable to treat ocular inflammation. Nanoparticles encapsulating an antibiotic drug, ofloxacin, were fabricated using emulsion solvent evaporation technique adopting 2^3 full factorial design to evaluate the effect of formulation parameters: that is to say, the molecular weight of the polymer (polycaprolactone), amount of Kolliphor P188, and presence of the charge inducer (chitosan hydrochloride) on the measured responses: drug entrapment efficiency (EE%), particle size (PS), polydispersity index (PDI) and zeta potential (ZP). The results show that the optimized LPCL-NP2 formulation (composed of low molecular weight polycaprolactone, 500 mg of Kolliphor P188, 0.25% chitosan hydrochloride, and 50 mg ofloxacin) displayed a sphere shape with EE%, PS, PDI, and ZP values of 89.73 ± 0.04%, 195.4 ± 13.17 nm, 0.323 ± 0.01, and 55.4 ± 0.66 mV, respectively. DSC study confirmed the amorphous nature of the drug. The optimized nanoparticle formulation was then further incorporated into the following two ocular formulations: gel (LPCL-NP2-G4) and in situ forming gel (LPCL-NP2-ISG4). The penetration of optimized ocular formulations was assessed by confocal laser scanning microscopy. The antimicrobial study was conducted for the following three ocular formulations: LPCL-NP2 presented as eye drops, LPCL-NP2-G4, and LPCL-NP2-ISG4 as well as the market product using rabbits which were infected in their eyes with *Escherichia coli*. Results revealed that rabbits treated with LPCL-NP2-ISG4 demonstrated a remarkable antibacterial efficacy and evident low bacterial growth which was additionally assured by the histopathological examination of eye biopsies compared with the other investigated groups. Thus, a novel ofloxacin-loaded nanoparticle formulation based on polycaprolactone is presented in the form of mucoadhesive non-irritating in situ forming ocular gel possessing a superior antibacterial activity.

Keywords Polycaprolactone · Ocular drug delivery · Ofloxacin · Nanoparticles · Mucoadhesive · Confocal laser scanning microscopy

Introduction

Being particulate carriers with a size of less than 1 μm where the drug can be dissolved, entrapped, encapsulated, or attached to their surfaces, nanoparticles (NPs) comprise potential drug delivery devices. They possess unique advantages, such as drug targeting to specific sites (through manipulation of their particle size and surface characteristics), controlling drug release at the target site to achieve maximum therapeutic efficacy and minimum adverse effects, as well as modulating the characteristics and degradation of the particles through the selection of matrix constituents to manipulate drug release according to the desired routes of administration [1, 2].

Among the routes of administration that NPs can be manipulated to achieve a great therapeutic impact is the ocular

✉ Mona M. AbouSamra
m_mona14@hotmail.com; mm.samra@nrc.sci.eg

[1] Pharmaceutical Technology Department, Pharmaceutical and Drug Industries Research Division, National Research Centre, 33 El-Buhouth Street, Dokki, Cairo 12622, Egypt

[2] Department of Pharmaceutics, Faculty of Pharmacy, Ahram Canadian University, 6th of October City, Cairo, Egypt

[3] Chemistry of Natural and Microbial Product Department, Pharmaceutical and Drug Industries Research Division, National Research Centre, Cairo 12622, Egypt

[4] Electron Microscopy Research Department, Theodor Bilharz Research Institute, Cairo, Egypt

route. It has been always known that many obstacles can face the conventional medications for the ophthalmic drug delivery represented by the reduced diffusion through reflex of blinking and the relevant effect of tear turnover or the possibility of binding to proteins besides the non-productive absorption through the conjunctiva [3]. Thus, designing a corneal-targeted controlled-release delivery system based on polymeric NPs can be promising to achieve a widely spaced dosing schedule with improved efficiency of therapy and patient compliance.

Ofloxacin (OFX) is a potent broad-spectrum antibiotic belonging to the second-generation fluoroquinolone with a noticeable effect against Gram-positive and Gram-negative bacteria [4]. It can be applied via the ocular route infections from numerous anaerobes, various species of *Staphylococcus*, as well as Chlamydia species [5]. Still, significant loss of the bioavailability, that can reach up to 90%, is attained following the application of topical ocular drugs owing to the previously mentioned problems [3, 6].

Among the commonly used polymers as a drug delivery matrix, polycaprolactone (PCL) attained great attention lately because of its biocompatibility and biodegradability [7]. PCL could be used as either a single polymer or in polymer blends with others [8]. Besides being cheap, soluble in a wide range of solvents with low melting point [3], PCL has been reported to possess good controlled release and optimum drug loading capability [9, 10], with excellent stability [11]. However, the major restriction of the ocular application of PCL-based NPs is their rapid clearance from the eye surface resulted from their negatively-charged surfaces [3]. Such a problem can be solved by coating PCL NPs by a mucoadhesive positively charged polymer, like chitosan. Chitosan and its derivatives are noticeably explored in many types of research for modification and improvement of different delivery systems [12, 13]. The main reason for CS selection is due to its cationic nature as well as its distinguished mucoadhesive properties. The surface medication of NPs by applying a coat of CS can guarantee a sustained retention time at the desired site of action and hence could result in a greater improvement of drug bioavailability [14].

Therefore, in the current study, the beneficial advantages of NPs were exploited and OFX was successfully entrapped in PCL NPs. Surface modification with CS-HCl was performed to enhance targeting and prolonging adherence at the eye surface. The prepared NPs were subjected to in vitro, ex vivo, and in vivo evaluations.

Materials and methods

Materials

Ofloxacin (OFX) was kindly provided from Rameda Pharmaceuticals, 6th of October City, Giza, Egypt. Polycaprolactone (Mwt 14,000), polycaprolactone (Mwt 45,000), Kolliphor P188, Pluronic F127, and cellulose membrane (molecular weight cut-off 12,000-14,000 g/mol) were purchased from Sigma-Aldrich, USA. Chitosan hydrochloride (CS HCl) was a generous gift from Zhejiang Chemicals Import & Export Cooperation, China. Methocel, fructose, sodium citrate, as well as buffer-forming salts were purchased from Sisco Research Laboratories Pvt. Ltd., India.

Methods

Preparation of OFX-loaded nanoparticles

OFX-loaded NPs were prepared by the emulsification solvent evaporation technique [15] adopting a 2^3 full factorial design. Specific weights of OFX (0.15% w/v) and PCL (0.75% w/v) were dissolved in dichloromethane. Kolliphor P188 was dissolved in deionized water in two different concentrations (2.5 to 5% w/v). The emulsion was formed as the organic phase was slowly dropped into the aqueous one with the aid of a homogenizer. The resulted emulsion was subjected to rotary evaporation under vacuum at 60 °C, and the rest of the organic solvent was evaporated [16, 17]. PCL-based nanoparticulate systems were prepared based on a 2^3 full factorial experimental design where the impact of various formulation variables was clearly revealed and an optimum formula can be easily detected; this was achieved with the aid of Design-Expert®-8 Software. Three factors (PCL molecular weight, concentration of Kolliphor P188, and presence or absence of CS HCl) were evaluated, each at two levels. The dependent parameters included particle size, zeta potential, and encapsulation efficiency. The detailed description of OFX-loaded NP composition is presented in Table 1.

Evaluation of the prepared nanoparticles

Assessment of the size and zeta potential The average size and surface charges of the prepared NPs were estimated using a Zetasizer (Malvern Instrument, Worcestershire, UK). Dilution of the dispersion with deionized water is a must before analysis. Three measurements were conducted at a fixed angle of 90° at room temperature for each sample, and the average was recorded.

Drug entrapment assessment The prepared formulations were centrifuged under cooling using a large capacity refrigerated centrifuge (Union 32R, Korea) for 1 h at 9000 rpm. The determination of the amount of OFX entrapped within the NPs was performed in an indirect way by calculating the concentration of free drug which remained dispersed in the separated supernatant media applying the following equation [18–20]:

Table 1 Composition of OFX-loaded PCL nanoparticles

Formula	PCL (mol wt)	Conc. of Kolliphor P188 (mg)	CS HCl (%w/v)
LPCL-NP1	14,000	500	–
LPCL-NP2			0.25
LPCL-NP3		1000	–
LPCL-NP4			0.25
HPCL-NP5	45,000	500	–
HPCL-NP6			0.25
HPCL-NP7		1000	–
HPCL-NP8			0.25

$$\text{Entrapment efficiency}\ (\%) = \frac{\text{Total amount of OFX} - \text{amount of free OFX}}{\text{Total amount of OFX}} \times 100$$

In vitro OFX release study In vitro release of OFX from the prepared formulations was assessed by the previously reported dialysis bag diffusion technique [21]. The cellulose dialysis bags (1 cm width and 7 cm length) were ready for use after an overnight soaking in the release media. A definite volume of OFX-loaded PCL NPs (2 mL) was filled within the dialysis bags with a secured closure of their ends. Bags were inserted in vials filled with 25 mL of phosphate buffer (pH 7.4) and subjected to thermostatically controlled shaking at 100 rpm/min maintained at 37 ± 1 °C [22, 23]. At predetermined time intervals, the concentration of drug was estimated from withdrawn samples by a spectrophotometrical assay at 288 nm. The release medium remained at a constant volume by replenishing the withdrawn samples with fresh ones. The release experiment was performed in triplicate. To understand the mechanism and kinetics of OFX released from the prepared NPs, the data were fitted using linear regression equations where the drug-release order was recorded.

Optimization An optimum formula exhibiting desirable characteristics demonstrated in possessing the smallest particle size, highest zeta potential, and entrapment efficiency values; as well as sustained in vitro drug release profile with reasonable release efficiency was selected for further studies.

Assessment of particle morphology The morphology of the selected NP formulation was manifested using TEM (JEOL, JEM-1230, Tokyo, Japan). One drop of the diluted sample was inserted on a standard formvar carbon-coated copper grid (200 mesh F/10 nm C/3–4 nm, Electron Microscopy Sciences). Staining was performed with 2% (w/v) phosphotungstic acid before examination. The photo was captured at suitable magnification power (X9000).

X-ray powder diffraction X-Ray powder diffraction (XRPD) pattern of OFX, PCL, CS HCl, and optimized OFX-loaded NPs were examined using X-ray diffractometer (Scintag Inc., USA). Irradiation of the samples was performed using Ni filtered, CuKa radiation at certain conditions (45 kV voltage, 2θ diffraction angle, and a 9 mA current at a scanning rate of 1° min^{-1} with 2θ diffraction angle over a range of 0 to 90°.

Differential scanning calorimetry The thermal characteristics of selected NP formulation along with its components were determined by differential scanning calorimetry DSC131 evo (SETARAM Inc., France). Standards of mercury, indium, tin, lead, zinc, and aluminum were used to calibrate the instrument. N_2 and He were exploited as the purging gasses. Instruments were programmed to heat the zone from 25 to 300 °C with a heating rate 10 °C/min. Weighed samples (5 mg) in aluminum crucible 120 μL were introduced to the instrument. The thermogram results were processed using CALISTO data processing software v.149. Any shift or disappearance/appearance of peaks was recorded.

Preparation of the topical ophthalmic formulations

Two subsequent formulations were developed from the selected NP formulation, namely, temperature-triggered in situ gelling system and a preformed gel.

Preparation of temperature-triggered in situ gelling system containing OFX-loaded PCL NPs The in situ gelling system was prepared by mixing the selected OFX-loaded PCL NPs containing 0.15% (w/v) OFX with (15, 18, 20, and 22% w/v) pluronic F127. Different concentrations of pluronic F127 were dissolved in deionized water by cooling and then kept at room temperature [18].

Preparation of gel system containing OFX-loaded PCL NPs The optimized PCL NPs were mixed with methylcellulose polymer in different concentrations (0.5, 1, 2, and 3% w/v). In brief, methyl cellulose (MC) gel bases were prepared by dispersing different amounts of the polymer in distilled water with the help of a magnetic stirrer until homogenous dispersion. The dispersion was kept for 48 h in the refrigerator to obtain a transparent solution. LPCL-NP2 was added to the MC solution with the incorporation of 10% w/v fructose.

Characterization of topical ophthalmic formulations

Determination of formulation pH About 0.5 g of the selected OFX-loaded NPs and its corresponding gel and in situ gelling system were diluted with distilled water to a volume of 10 mL. The pH values were estimated at 25 °C by a digital pH meter (Jenway, Bibby Scientific Limited, Staffordshire, UK) previously standardized using buffer solutions (pH 7.0 and 10.0). All measurements were performed in triplicate.

Rheological study The flow curves of prepared and in situ gels were obtained using a computerized rheometer equipped with a cone and plate at 37 °C (plate diameter at 40 mm, cone angle at 4°). Continuous variation of the speed rate, for each sample, from 1 to 100 s^{-1} and then backward from 100 to 1 s^{-1} was applied, and the resulting viscosity was recorded.

In vitro drug release studies The in vitro release of OFX from the studied formulations (the optimized OFX-loaded PCL NPs as well as from the corresponding gel and in situ gel) was evaluated using the dialysis bag diffusion technique as reported by Yang et al. [24]. Regarding 25 mL of phosphate buffer, pH 7.4 was used as release medium. The sample was placed into a cellulose acetate dialysis bag (molecular weight cutoff 12,000–14,000) sealed at both ends and immersed in the buffer. Samples were stirred at 100 rpm, and maintained at 37 ± 1 °C [25, 26]. At predetermined time intervals, samples were withdrawn from the release medium and assayed spectrophotometrically at 288 nm. Each withdrawn sample was replaced by an equal volume of fresh release medium.

Microbiological studies

Sterility study Plain ophthalmic dosage forms and others containing OFX were inoculated on blood agar medium, composed of Tryptic soy agar (TSA, Difco), containing rabbit blood (5% v/v), and eosin methylene blue. A suspension of standard *Escherichia coli* was seeded in the prepared agar plates. After an incubation period of 48 h at 37 °C, examination of the media was performed seeking evaluation of the bacterial colony count.

Antibacterial activity study Evaluation of the antimicrobial activity of the studied formulation was done through the disc diffusion method [27]. Healthy, male albino rabbits weighing about 2.5 to 3.0 kg were utilized in this study after getting the required approval from the Animal Ethics Committee of the National Research Centre (NRC) (approval number: 16142). All of the guidelines established by the NRC for taking care and use of laboratory animals were taken into consideration. The animals were freely allowed to standard food and water.

Rabbits were infected in their eyes with *Escherichia coli* where the antimicrobial activity of the studied formulations was compared with the marketed eye drop product Oflox®. The study was performed via insertion of sterile diameter filter paper discs (6 mm, Whatman no. 1) under the eyelid for 1 min at predetermined time intervals (0.5–6 h) after a single installation (50 μL) of the studied formulations each in the right eyes of six rabbits (conjunctival sac region). Then, the discs were inserted in the nutrient broth tubes inoculated with 100 μL of the bacterial suspension. The inoculated broth was then incubated at 37 ± 0.5 °C for 24 h where the inhibition of bacterial growth was estimated by measuring the cultures' optical density using a UV spectrophotometer at 600 nm. Percentage of inhibition, which is related to the level of drug in the eye tears following the topical application of tested drug formulae, was calculated using the NB medium inoculated with *Escherichia coli* as control.

The growth inhibition percent (%) was calculated according to the following equation [28]:

$$[(A_c - A_s)/A_c] \times 100$$

where A_c is the optical density of control and A_s is the optical density of the sample.

Corneal visualization using confocal laser scanning microscopy

The penetration of fluorescently labeled formulations through the cornea was assessed using invert confocal laser scanning microscopy (CLSM) (LSM 510 Meta, Carl Zeiss, Jena, Germany). Rhodamine B (RhB; a fluorescent dye) was chosen to simulate the incorporated drug. To achieve this target, RhB-loaded PCL NPs were prepared applying the same technique employed for preparing OFX-loaded PCL NPs but with a 0.15% w/v concentration of RhB, replacing OFX in the prepared formulations. One drop of each of the studied systems (RhB-loaded PCL NPs) and its incorporated form within gel and in situ gel formulations was applied every hour, 6 times in all. When all of the instillations were over, an intravenous injection of an overdose of sodium pentobarbital was given to rabbits to euthanize them through the marginal ear vein. Isolation of corneas and rinsing in physiological saline were done to prepare the samples for mounting on glass slides and subsequent observation by CLSM. For confocal imaging, a CLSM system (TCS SP2/AOBS, Leica, Germany) linked to an inverted microscope with a HCX PL APO 100, 1.40–0.70 oilCS objective) (DM IRE2, Leica, Germany) was used. Excitation lasers of Ar and HeNe (excitation 485 and 595 nm, respectively) were the best for RhB. LEICA confocal software version 4.2 (Carl Zeiss microimaging, Gottingen, GMBH) was used to process image acquisition and analysis [21, 29].

Histopathological examination

Each intact eye globe was fixed in 10% neutral buffered formalin. The fixative was adequately covering the eye. Horizontal sections passing by the cornea were taken for histological examination after 24 h. Two parallel horizontal cuts were made. The samples were immersed in 10% buffered formalin for 24 h at room temperature and processed for paraffin embedding. The ocular tissue was thoroughly dehydrated in a graded ethanol from 50, 60, 70, 90–95, and 100% to avoid distortion of the tissue, and the water in the specimen was gradually replaced by the alcohol and then cleared using two bathes of xylene. Dehydration and clearing were performed at room temperature and then followed with liquid paraffin infiltration. The tissue was embedded in the correct orientation on its edge in the mold to permit examination of all corneal thickness [30]. Four micrometer-thick sections were done using a microtome (Leica HistoCore BIOCUT). The obtained tissue slides were stained with hematoxylin and eosin (H&E) [31]. The structure was observed under the light microscope (Leica, DM-6000, Wetzlar, Germany) with integrating camera for histopathological changes.

Stability study

To perform the study, an adequate storing of the selected OFX-loaded NP formulations in sealed amber colored glass vials at refrigerator temperature (2–4 °C) was assured in a dark environment for 9 months. At predetermined time intervals of storage (after 3, 6, and 9 months), both assessing of the physical appearance as well as analyzing critical formulations' parameters concerning drug entrapment efficiency, particle size, PDI, and zeta potential were performed and compared with fresh formulations [32, 33]. The experiments were performed in triplicate.

Statistical analysis

The statistical analysis of the obtained data ($n = 3$) was performed using a validated statistical program (SPSS®-17.0; SPSS Inc., Chicago, IL). P values of less than 0.05 were considered statistically significant after determining the significance of differences by one-way analysis of variance (ANOVA) followed by the least significant difference test.

Results and discussion

Emulsification solvent evaporation is a successful method for preparing PCL NPs. As indicated by its name, the method comprises two steps; emulsion formation and then solvent evaporation. First, in the emulsion step, an organic phase containing the polymer dissolved in a suitable organic solvent is emulsified in an aqueous phase (containing a suitable surfactant) to produce a simple O/W emulsion. Then, in the solvent evaporation step, the resulting "oil" droplets were solidified as the organic solvent was removed by evaporation leading to the precipitation of the polymer around the droplets, and hence, solidified particles were produced. The solvent evaporation process in this article was carried out in a rotary evaporator where the increased temperature and reduced pressure promoted the evaporation process.

Preparation of OFX-loaded nanoparticles

OFX-loaded PCL NPs were successfully prepared using the emulsion solvent evaporation technique. Kolliphor P188 was used as the surfactant for completing the emulsification process. It is a non-ionic surfactant approved by the FDA. It can act as both an emulsifier and a co-emulsifier in the nanoparticle manufacture procedure, resulting in smaller particle sizes with small PDI [34]. As a stabilizer, it can offer an extra steric stabilization effect through preventing fine colloidal particles from aggregation in their system. Smaller particles are often produced when Kolliphor P188 is specifically used [35].

Evaluation of the prepared nanoparticles

Measurement of particle size and zeta potential

Values of particle size, polydispersity index, and zeta potential are shown in Table 2. It can be demonstrated that particle size of the prepared PCL NPs is affected by the grade of PCL used, the concentration of surfactant, and the presence of CS-HCl (Fig. 1a). The increasing molecular weight of PCL from 14,000 to 45,000 caused a significant increase in NP size (Fig. 1a). This can be explained by the increased viscosity of the polymer solution as a function of its concentration or its molecular weight of the polymer. Consequently, higher molecular weight polymer solutions are expected to yield larger nanoparticle sizes at a fixed concentration of the same polymer [36].

As demonstrated in Table 2 and Fig. 1b, increasing Kolliphor P188 concentration from 500 to 1000 mg caused a significant increase in NP size ($p < 0.05$); this was perceived upon comparing each formula against its analogue with higher Kolliphor content. This could be explained by the accumulation of more surfactant molecules within the formed NPs as well as their surfaces. The increase of the number of polymer chains per unit volume can lead to more massive structures producing larger particle size [37].

Moreover, a significant increment in PCL NP sizes was recorded upon addition of CS-HCl ($p < 0.05$) (Fig. 1c). This can be related to the adsorption and deposition of CS-HCl molecules on the surface of the prepared NPs as well as the

Table 2 Particle size, PDI, zeta potential, and entrapment efficiency values for the prepared OFX-loaded PCL NPs

Formula	Particle size (nm) ± S.D.	PDI ± S.D.	Zeta potential (mV) ± S.D.	EE (%) ± S.D.
LPCL-NP1	78.41 ± 4.73	0.141 ± 0.004	0.536 ± 0.02	71.12 ± 1.94
LPCL-NP2	195.4 ± 11.80	0.323 ± 0.008	55.4 ± 3.07	89.73 ± 3.09
LPCL-NP3	139.6 ± 9.11	0.477 ± 0.009	− 0.836 ± 0.03	58.52 ± 1.80
LPCL-NP4	347.2 ± 22.14	0.588 ± 0.010	59.4 ± 2.33	92.1 ± 2.00
HPCL-NP5	220 ± 11.01	0.536 ± 0.018	− 0.592 ± 0.01	60.00 ± 0.89
HPCL-NP6	473.5 ± 15.34	0.701 ± 0.020	46.3 ± 2.23	93.16 ± 1.36
HPCL-NP7	319.6 ± 10.10	0.385 ± 0.007	− 0.677 ± 0.03	65.70 ± 0.98
HPCL-NP8	513.9 ± 16.43	0.677 ± 0.02	43.3 ± 2.03	85.59 ± 4.21

increased viscosity of the resulting prepared solution which affects the produced NP size [37]. The PDI of the prepared NP formulations indicates good homogeneity and narrow size distribution [38, 39].

Zeta potential of the NP formulations prepared with CS-HCl (LPCL-NP2, LPCL-NP4, HPCL-NP6, and HPCL-NP8) showed positive charges with significantly elevated values that might be attributed to the deposition of cationic molecules of CS-HCL on the surface of the PCL NPs (Fig. 1d).

Drug entrapment assessment

Results of entrapment efficiencies of the prepared PCL NP formulations are displayed in Table 2. The values of OFX-EE ranged from 58.52 to 93.16%. The promising high EE values obtained for all formulations can be related to the similar hydrophobic nature of both OFX and PCL, which facilitates integrating of OFX within the PCL matrix. The values of EE were increased significantly upon incorporating CS-HCl (Fig. 1e). This was observed when comparing each single formulation versus its equivalent one containing CS-HCl. The formed coating of PCL NPs by CS HCl can prevent the escape of OFX and thus yielding high EE values.

In vitro OFX release study

Plotting the cumulative percentage of OFX released from the prepared PCL NPs against time was used to give an insight on their release patterns. As depicted in Fig. 2, sustained release profiles were obtained over 6 h. The results reveal a slower release of OFX from various PCL NP formulations. It can be depicted that the release of OFX was controlled by PCL polymer which ensures steady and effective absorption of OFX. A biphasic drug release pattern was noticed, where the initial burst release of OFX was related to the immediate dissolution of OFX adsorbed on the surface of the NPs as well as the hydrophilicity (HLB = 29) of Kolliphor P188 which lead to the formation of porous surfaces of PCL NP structure [40]. Then, a slow and sustained release phase of OFX is obtained from the drug reservoir present on the polymer matrix core [41]. The release pattern integration of the investigated formulations follows mostly the Higuchi's model. This finding proves that the systems under investigation followed the matrix diffusion–based release kinetics.

Optimization of formulation variables

The experimental design is mainly exploited to survey the effect of the studied variables on the resulted selected responses aiming to recognize the optimum level for each factor [42]. The main objective is to produce an optimized formulation with a given set of restrictions to achieve a robust product with highly favorable characteristics [43]. In the present study, Design Expert® 8 software through graphical and numerical analyses suggested the NP formulation LPCL-NP2 (composed of low molecular weight PCL, 500 mg Kolliphor P188, and CS-HCl) to be the optimum one with a desirability value of 0.949.

Transmission electron microscopy

Morphology of the selected NP formulation was examined using transmission electron microscopy (TEM). NPs are shown in Fig. 3. Micrograph reveals fine detached homogenous NPs, sphere-shaped with dense structure and soft surfaces appearing as black dots.

X-ray powder diffractometry

As known that each material has a specific pattern as a fingerprint, XRPD is utilized for the identification of substances forming any compound. XRPD studies were performed to examine the changes in the crystallinity and nature of OFX-loaded NPs. The XRPD patterns of OFX, PCL, CS-HCl, and LPCL-NP2 are clarified in Fig. 4. As clearly seen in the figure, OFX revealed intense characteristic peaks, both CS-HCl and PCL revealed two sharp peaks for both of them at $2\theta = 20$ and 23.1 °C and at $2\theta = 23.2$ and 24.6 °C, respectively. On the other hand, X-ray pattern of LPCL-NP2 showed an amorphous nature as verified by the loss of the individual sharp peaks of all composing materials [44]. The obtained data illustrated the possible interaction between OFX and the other

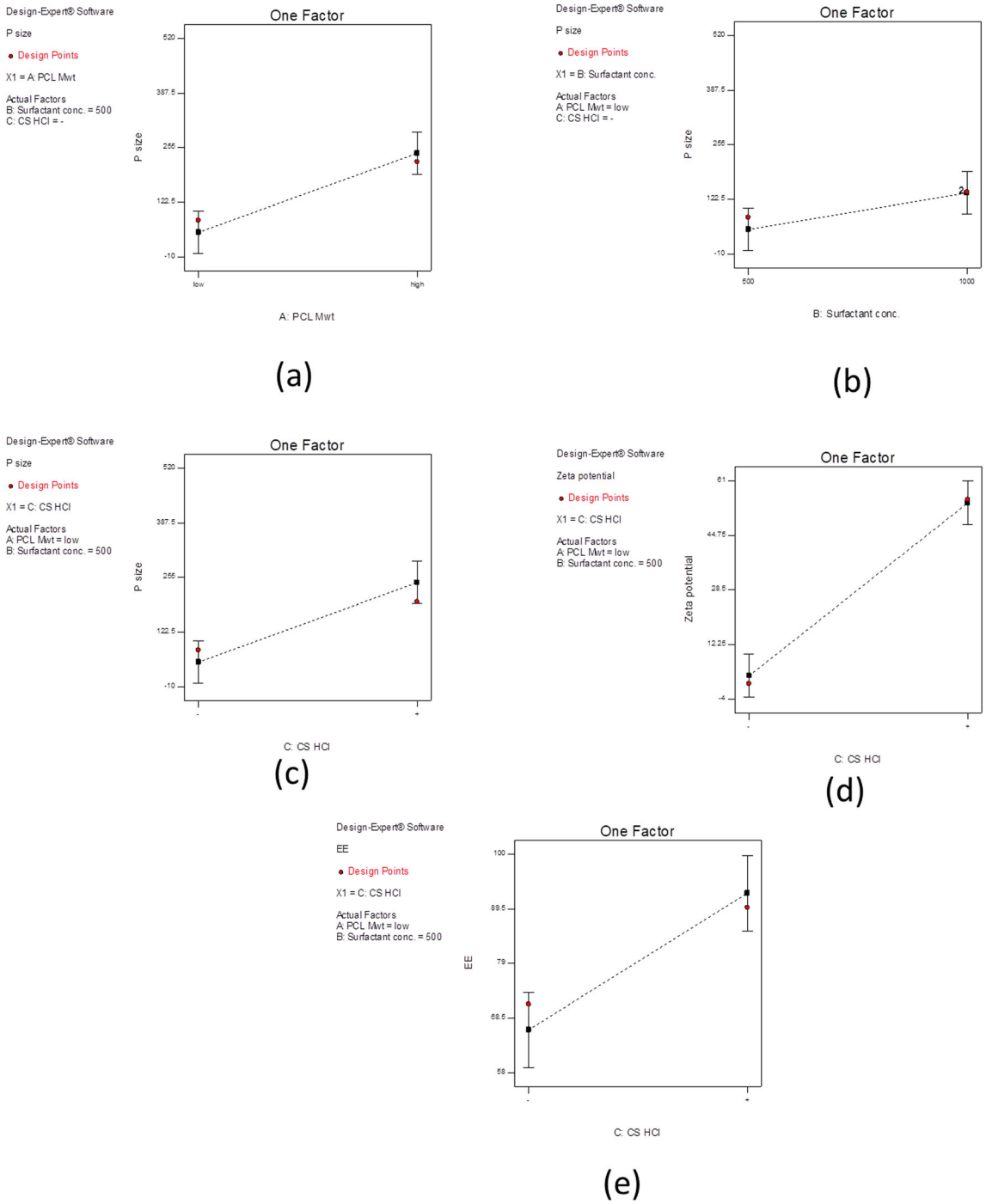

Fig. 1 Design expert plot showing the significant formulation variables on particle size (**a**, **b**, and **c**), zeta potential (**d**), and EE (**e**)

components and subsequent encapsulation of the drug in the formed NPs which resulted in the loss of its crystallinity.

Differential scanning calorimetry

The thermal characteristics of LPCL-NP2 formulation along with its components were determined by differential scanning calorimetry (DSC). DSC thermograms of OFX, PCL, CS-HCl, Kolliphor P188, and LPCL-NP2 are demonstrated in Fig. 5. As shown, OFX displays a sharp endothermic peak at 276.92 °C which is attributed to drug melting and indicates its crystallinity [45]. Equally, the DSC thermograms of PCL, Kolliphor P188, and CS-HCl show endothermic peaks at 59.9, 52.44, and 201 °C, respectively, which correspond to their melting temperature points. Conversely, the thermogram of LPCL-NP2 showed the lack of the characteristic peaks of both OFX and PCL demonstrating that OFX was completely dispersed inside the created NPs and proving transforming the

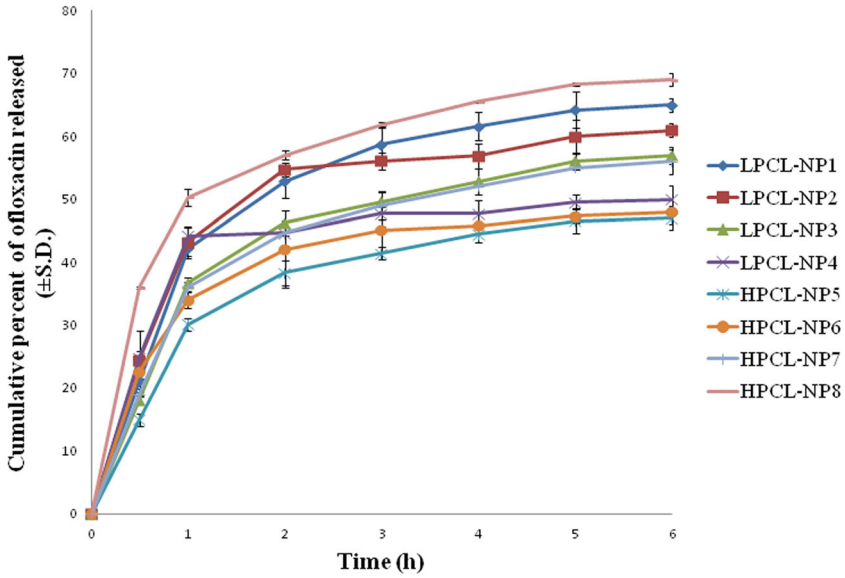

Fig. 2 Release profiles of OFX from the investigated PCL NPs

drug to an amorphous form as well as its incorporation within the NPs.

Preparation of the topical ophthalmic formulations

Two formulations were developed from the selected LPCL-NP2 formulation, namely, temperature-triggered in situ gelling system and a preformed gel.

Preparation of temperature-triggered in situ gelling system containing OFX-loaded PCL NPs

An essential property for the ocular in situ gel system is to be low-viscous free flowing liquid at non-physiological temperature to be administered easily as eye drops but undergo in situ phase transition to transform to a gel which can tolerate the shear forces in the cul de-sac and control the drug release at physiological condition [46]. As shown in Table 3, formula LPCL-NP2-ISG4 containing pluronic F127 in a final concentration of 22% demonstrated the best in situ gel transformation and thus was selected for further studies.

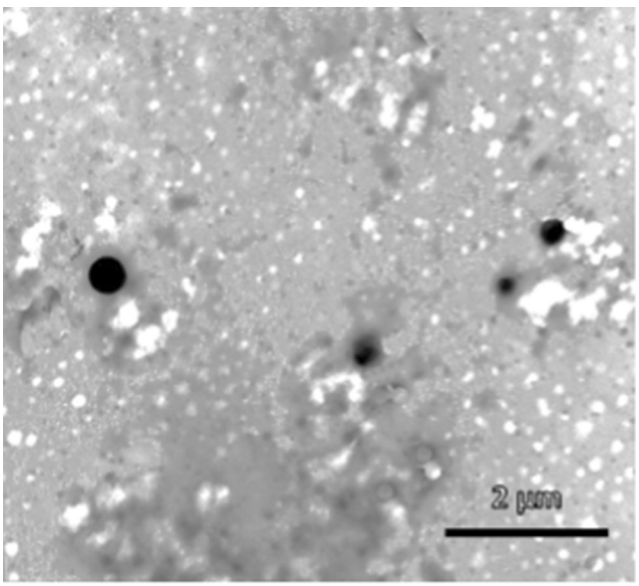

Fig. 3 Transmission electron micrograph of the optimized formulation

Preparation of gel system containing OFX-loaded PCL NPs

A combination of two polymers, namely methyl cellulose (MC) and fructose in different concentrations, and their impact on the degree of gelation were investigated (Table 4). The best degree of gelation was manifested upon mixing 3% w/w MC and 10% fructose (LPCL-NP-G4). A high gelation temperature was recorded due to the low intermolecular hydrogen

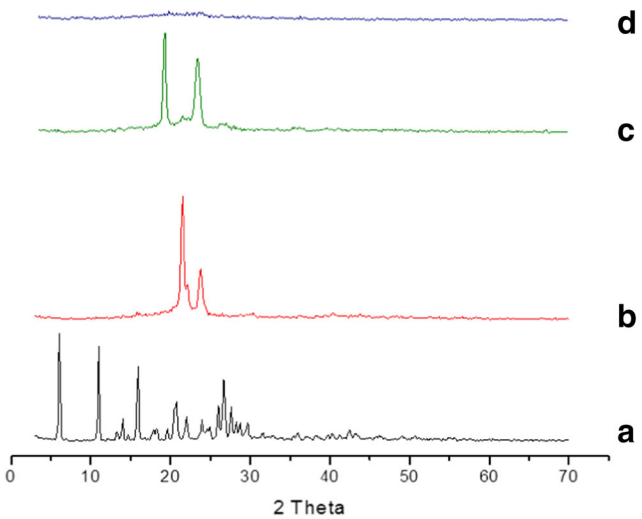

Fig. 4 XRP diffractograms of (**a**) OFX, (**b**) PCL, (**c**) CS-HCl, and (**d**) LPCL-NP2

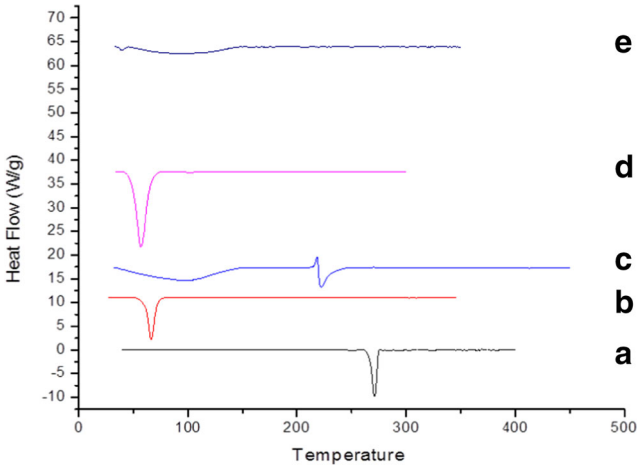

Fig. 5 DSC thermograms of (**a**) OFX, (**b**) PCL, (**c**) CS-HCl, (**d**) Poloxamer 188, and (**e**) LPCL-NP2

bonding between MC [47]. Moreover, fructose is a monosaccharide that increases the viscosity more rapidly compared with other sugars. Also, it is an outstanding humectant to keep moisture for an extended period even at conditions of low humidity [48].

Characterization of topical ophthalmic formulations

pH measurement

It is known that ocular annoyance and hurting sensation can result if the difference in the pH values of the instilled ophthalmic products and tear fluid is very far [49]. For this reason, the perfect pH for safe ophthalmic products should be equal to that of the tear fluid which is about 7.4 [50]. It was found that the pH of LPCL-NP2, LPCL-NP2-G4, and LPCL-NP2-ISG4 ranges from 7.3 ± 0.03 to 7.4 ± 0.01. These results are within the required range.

In vitro release of OFX from nanoparticle formulations

Figure 6 illustrates the data of OFX released from LPCL-NP2, LPCL-NP2-G4, and LPCL-NP2-ISG4. OFX exhibited a sustained release pattern from the investigated formulations which extended over 6 h. The data demonstrated that the inclusion of the LPCL-NP2 into the ocular gel or the in situ forming gel did not significantly affect the release rate of OFX, ensuring the appropriateness of incorporating the LPCL-NP2 inside the ocular gel or the in situ forming gel without affecting the intended drug release pattern.

Table 3 In situ gelling capacity of OFX-loaded PCL NP–based in situ gels prepared using different concentrations of pluronic F127

In situ gel system	Pluronic F127 (%w/v)	Degree of gelation[a]
LPCL-NP2-ISG1	15	–
LPCL-NP2-ISG2	18	–
LPCL-NP2-ISG3	20	+
LPCL-NP2-ISG4	22	++

[a] Grades of gelation: (−) no gelation, (+) slow weak gelation, and (++) immediate stiff gelation which lasts for extended period of time

Rheological behavior The rheological properties of the optimized ocular formulations are presented in Fig. 7 by plotting the shear rate versus the viscosity (flow curve). The rheological behavior of the in situ gel formulations (LPCL-NP2-ISG4) exhibited pseudoplastic flow characteristics (shear thinning systems). It was found that the viscosity increases at low shear rates and decreases under conditions. This is an advantageous characteristic of shear-thinning systems in displaying greater viscosity in the open eye, stabilizing the tear film which is preferred commercially [51]. Same rheological property was depicted for the LPCL-NP2-G4 formulation in displaying a non-Newtonian flow where a shear thinning behavior was recorded. It had been reported that a gel formulation can be stored at any temperature showing unchangeable viscosity, and for this reason, it is characterized by its high stability [52]. However, it may lead to blurred vision as well as foreign body sensation when applied on the eye surface [53].

Microbiological studies

Antibacterial activity study

The antimicrobial effect of LPCL-NP2, LPCL-NP2-ISG4, and LPCL-NP2-G4 compared with the marketed eye drop Oflox® was evaluated after their application on the infected rabbit's eye with *E. coli*.

LPCL-NP2-ISG4 showed a remarkable effect since the second hour until the third hour, a plateau formation during the period of treatment was noticed (Fig. 8).

The significant difference shown by LPCL-NP2-ISG4 in its antibacterial activity compared with LPCL-NP2 and the market product returned to the prospective advantage of vesicular carriers to come in close contact with the surfaces of cornea and conjunctiva, accordingly, raising the prospect of ocular drug absorption [54]. Moreover, the gelling capability of agglutinating to the eye tissues leads to a prolonged OFX effect.

Corneal visualization using confocal laser scanning microscopy

Figures 9 (a–c) Illustrate the transcorneal penetration of the tested formulations using rhodamine B (RhB) dye–loaded LPCL-NP2, LPCL-NP2-G4, and LPCL-NP2-ISG4.

Table 4 OFX-loaded PCL NP–based gel formulations

Gel system	Methyl cellulose (% w/v)	Fructose (% w/v)	Degree of gelation[a]
LPCL-NP2-G1	0.5	10	–
LPCL-NP2-G2	1	10	–
LPCL-NP2-G3	2	10	+
LPCL-NP2-G4	3	10	++

[a] Grades of gelation: (−) no gelation, (+) slow weak gelation, and (++) immediate stiff gelation which lasts for extended period of time

RhB-LPCL-NP2 applied to the normal eye revealed uniform penetration of the dye all over the thickness of the corneal epithelium to the basement membrane and the limited area of the bowman's membrane (Fig. 9a). This finding can be related to the rapid washout of the formulation before the free drug release is completed. Meanwhile, RhB-LPCL-NP2-G4 irregularly penetrates the epidermal layer of the cornea and appeared limited to the superficial part of the corneal epithelium. The fluorescence took gelatinous appearance (Fig. 9b). This denotes that the gel formula faced a sort of ocular penetration resistance. It is known that the specific system of the eye components and organization grants a high resistance to all external materials, including ocular drug delivery [55, 56]. Although the RhB-LPCL-NP2-ISG4 revealed irregular penetration of the corneal epithelial surface, fluorescence reactions were disclosed all through the layers of the cornea, sclera, and conjunctiva (Fig. 9c). The fluorescence distribution was depicted all over the different corneal layers as well as the superficial epithelial layers, the basal epithelial layers, and the collagenous Bowman's layer. Moreover, the distribution of fluorescence all over the hydrophilic stroma was apparent. Besides, the intense fluorescence was found to spread through deeper corneal layers—the Descemet's membrane and the endothelium. The corneal permeation and the muco-adhesion measurements of the Rh-LPCL-NP2-ISG4 allowing prolonged residence time on the cornea favored intercellular and intracellular penetration to take place [57].

Histopathological examination

Histopathological examinations of corneal sections of the investigated rabbit's eye are displayed in Fig. 10 (a–f). The microscopic examination of the normal corneal biopsy showed a vascular corneal structure with thin continuous epithelial basement membrane, no break in the bowman's membrane with any inflammatory cells disclosed in the substantial propria apart from very few scattered lymphocytes between the normal collagenous lamellae. Also, the Descemet's membrane did not show any thickening or breaks as well the conjunctiva covering the anterior surface of the sclera showed intact epithelial surface and a loose vascular tissue (Fig. 10a). On the other hand, Fig. 10b presenting the corneal section of the infected untreated rabbit revealed signs of corneal ulcer in the form of thinned corneal epithelium at different sites, breaks in the corneal epithelial basement membrane resulting in tissue folding. Also, the section showed ulcerated areas with edematous sclera and conjunctiva with inflammatory cellular infiltration of ciliary body and dystrophy involving the endothelial layer of the cornea. On the contrary, infected treated eye with the LPCL-NP2 revealed intact corneal epithelium, well-formed collagenous tissue of the bowman

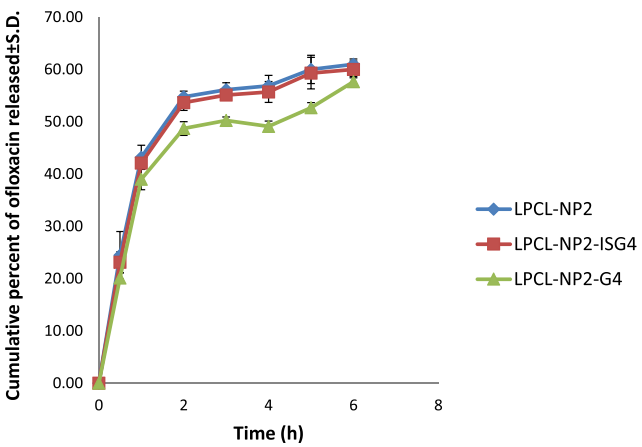

Fig. 6 Release profiles of OFX from the investigated LPCL-NP2, LPCL-NP2-ISG4, and LPCL-NP2-G4

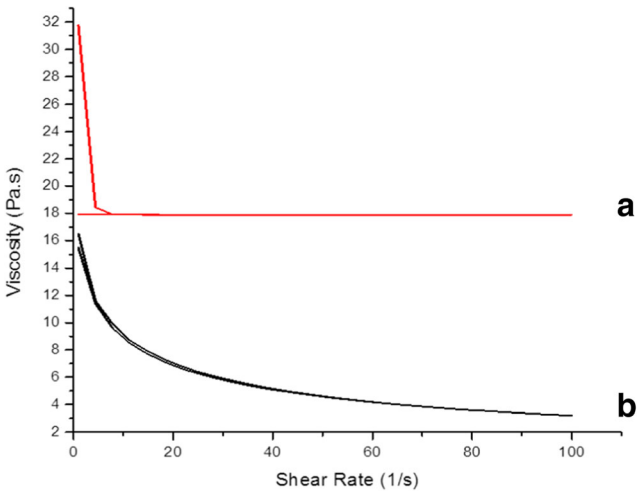

Fig. 7 Rheology profiles of LPL-NP2-G4 (**a**) and LPL-NP2-ISG4 (**b**)

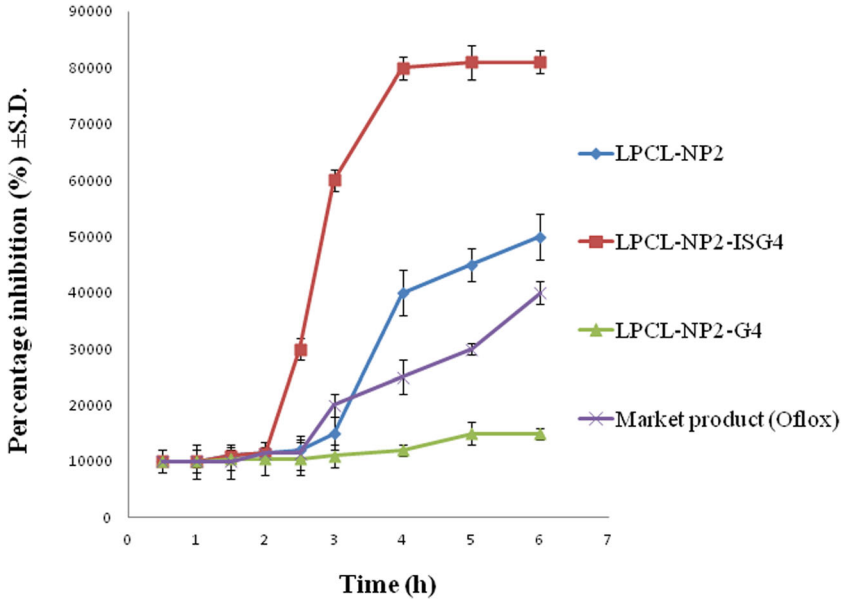

Fig. 8. Percentage inhibition of *Escherichia coli* growth produced by LPCL-NP2, LPCL-NP2-ISG4, and LPCL-NP2-G4 compared with Oflox® in the eyes of albino rabbits

membrane, corneal stroma comparable to the control section, intact Descemet's membrane, and few inflammatory cells scattered between collagenous lamellae of cornea and sclera. Meanwhile, edema of sclera and conjunctiva involving all the examined surface was noticed (Fig. 10c). The infected treated eye with the LPCL-NP2-G4 (Fig. 10d) disclosed sites of ulcerated cornea. The destructed epithelial layer in the case of the applied gel formula was deep, but no breaks were noticed in the epithelial basement membrane. The collagenous lamellae of the bowman membrane underneath the corneal epithelium appeared separated by moderate edema and inflammatory cells scattered in the cornea, sclera, and the

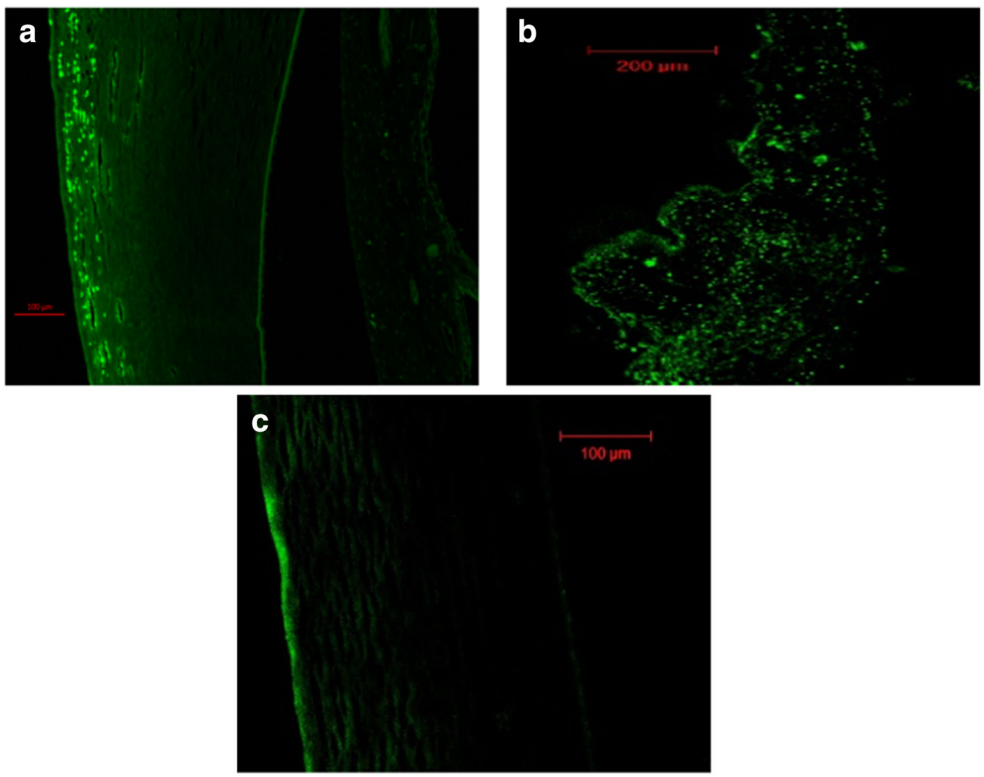

Fig. 9 CLSM images of RhB–loaded nanoparticle formulations after 2 h in vivo application on rabbit's eye. (**a**) LPCL-NP2, (**b**) LPCL-NP2-ISG4, and (**c**) LPCL-NP2-G4

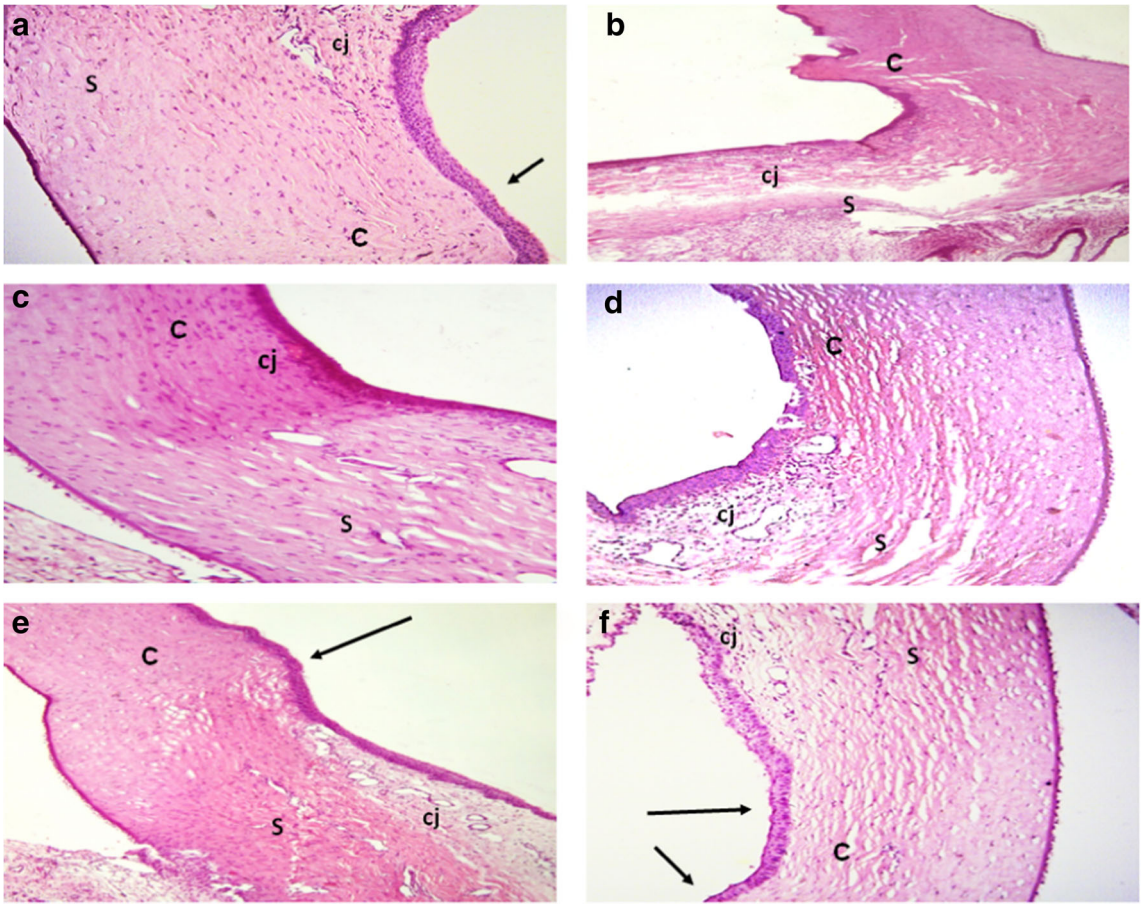

Fig. 10 Photomicrographs of histopathological study for the examined rabbits stained section with hematoxylin–eosin (H&E) of the cornea (C), conjunctiva (cj), and sclera (S) (magnification ×10) of (**a**) normal tissue architecture with normal lining epithelium (thick arrow), (**b**) infected tissue of the untreated eye, (**c**) corneal tissue that received Rh-LPCL-NP2, (**d**) corneal tissue that received Rh-LPCL-NP2-ISG4, (**e**) corneal tissue that received Rh-LPCL-NP2-G4, and (**f**) corneal tissue that received Oflox® (market product)

vascular conjunctival stroma. These pathological changes can be explained based on the revealed limited penetration of the corneal epithelium by the rhodamine dye–loaded NP gel formula (Fig. 9b). The detected histopathological changes in the infected treated eye with the LPCL-NP2-ISG4 were comparable with the changes denoted in LPCL-NP2 formula treated eye, but with mild noticed edema of the cornea and sclera. This limited edema pointed to minimize damage in the endothelial corneal layer in this tested group. It was reported that lack of effective pumping by the endothelial cells increases hydration of the corneal stroma, which disrupts the normally uniform periodic spacing of collagen fibrils [58]. Very fine undulation and redundancies of the bowman membrane at the site of localized corneal stromal edema were noticed (Fig. 10e). In the same time, the infected treated eye with the market product Oflox® revealed thinning of the corneal epithelium in some areas as results of superficial ulcer formation. Diffuse separated collagenous lamellae all over the corneal stroma and the sclera secondary to edema with inflammatory cellular infiltrate were depicted in the examined sections (Fig. 10f).

These findings are consistent with what is studied previously that the uses of low viscosity eye drop can be quickly cleared before the complete release of the drug. Thus, integrating OFX within NPs can overcome this drawback by acting as a reservoir, which is capable of defeating the rapid drug loss and washing out [59]. Additionally, the combination of the proposed LPCL-NP2 in an in situ gel could maintain the drug retention on the eye surface for successful convenience and improved permeation through ocular tissues [60].

Stability study

Over the study period, drug entrapment efficiency, particle size, and PDI, as well as physical appearance were assessed after 3, 6, and 9 months of storage and compared with fresh formulations. The stability results showed that entrapment efficiency, particle size, zeta potential, and PDI values for LPCL-NP2-ISG4 and LPCL-NP2-G4 did not change significantly over 9 months as shown in Fig. 11(a–d). Besides, no further precipitation or stratification was observed in the formulae during storage at 4 °C. However, LPCL-NP2 revealed a

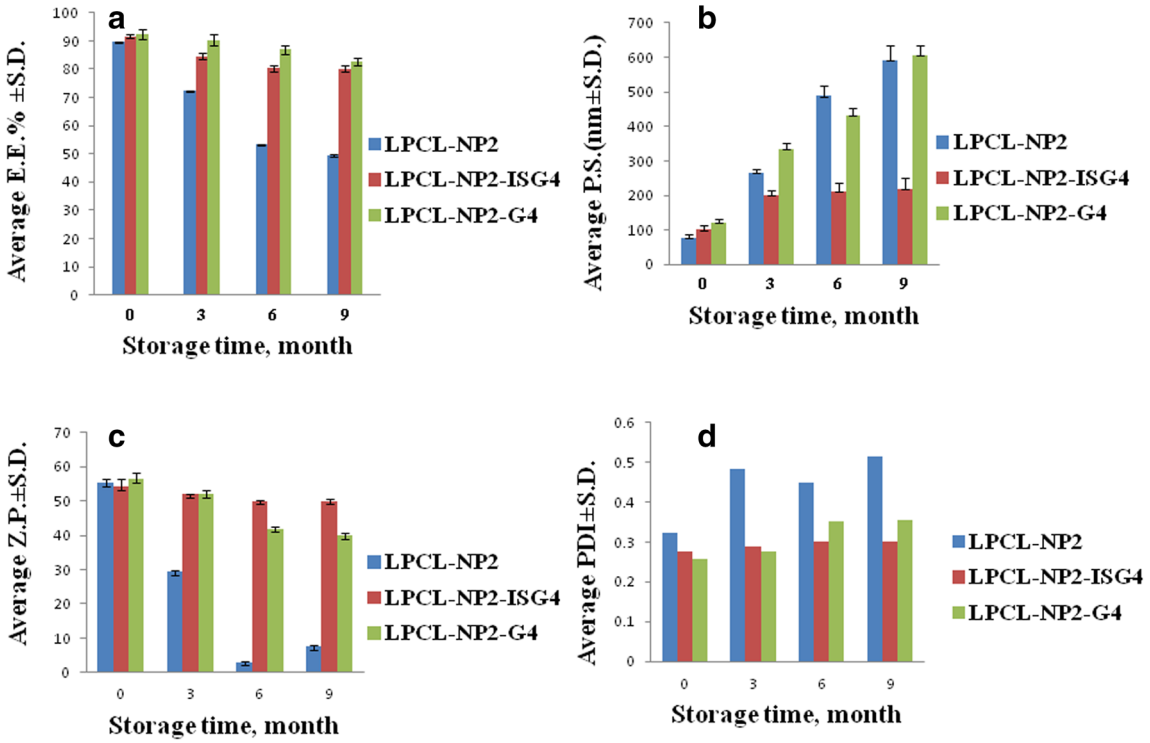

Fig. 11 Stability profile of LPCL-NP2, LPCL-NP2-ISG4, and LPCL-NP2-G4 during a storage of 9 months at 4 °C. (**a**) Changes in the entrapment efficiency (%). (**b**) Changes in the average particle size. (**c**) Changes in the average zeta potential. (**d**) Changes in the average polydispersity index

significant decrease in entrapment efficiency and zeta potential (Fig. 11a and c), respectively, accompanied with significant increase in both particle size and PDI values (Fig. 11b and d), respectively. Regarding these results, it can be hypothesized that OFX stability is best controlled in LPCL-NP2-ISG4 and LPCL-NP2-G4 formulations.

Conclusions

Our study has visualized the effectiveness of the innovative PCL NPs encapsulating the antibiotic drug, OFX using emulsion solvent evaporation technique. Low molecular weight PCL succeeded to formulate an optimum formulation (LPCL-NP2) showing small nano-sized particles with low PDI value, adequate positive zeta potential, and high entrapment efficiency. LPCL-NP2 was further incorporated in a preformed gel (LPCL-NP2-G4) as well in a temperature triggered in situ forming gelling system (LPCL-NP2-ISG4). The efficacy of LPCL-NP2, LPCL-NP2-ISG4, and LPCL-NP2-G4 formulae versus the market product Oflox® in inhibition of *Escherichia coli*–infected rabbit's eyes and the treatment of associating corneal ulcer were evaluated. The LPCL-NP2-ISG4 preparation revealed the maximum corneal, conjunctival, and scleral penetration seen by CLSM. The stability study performed for 9 months showed no significant changes concerning the entrapment efficiency, particle size, zeta potential, and PDI values regarding both the LPCL-NP2-ISG4 and LPCL-NP2-G4 formulations.

This study presents noninvasive innovative ocular drug delivery systems for OFX. The promising LPCL-NP2-ISG4 can enhance drug effectiveness by increasing ocular drug penetration and absorption. Moreover, it possibly will reduce drug administration frequency and improve patient compliance. Also, this study has highlighted the limited effectiveness of the gel formula for eye application.

Acknowledgments The authors acknowledge financial support from the National Research Centre through a grant (No: 11010301).

Compliance with ethical standards

Conflict of interest The authors declare that there are no conflicts of interest.

References

1. Woodruff MA, Hutmacher DW. The return of a forgotten polymer: polycaprolactone in the 21st century. Prog Polym Sci. 2010;35:1217–56.
2. Imbrogno A, Piacentini E, Drioli E, Giorno L. Micro and nano polycaprolactone particles preparation by pulsed back and-forward cross-flow batch membrane emulsification for parenteral administration. Int J Pharm. 2014;477:344–50.

3. Chandasana H, Prasad YD, Chhonker YS, Chaitanya TK, Mishra NN, Mitra K, et al. Corneal targeted nanoparticles for sustained natamycin delivery and their PK/PD indices: an approach to reduce dose and dosing frequency. Int J Pharm. 2014;477:317–25.
4. Nagayama A, Nakao T, Taen H. In vitro activities of ofloxacin and four other new quinoline-carboxylic acids against Chlamydia trachomatis. Antimicrob Agents Chemother. 1988;32:1735–7.
5. Gwon A. Topical ofloxacin compared with gentamicin in the treatment of external ocular infection. Ofloxacin Study Group. Brit J Ophthalmol. 1992;76:714–8.
6. Sayed EG, et al. Improved corneal bioavailability of ofloxacin: biodegradable microsphere-loaded ion-activated in situ gel delivery system. Drug Des Devel Ther. 2015;9:1427–35.
7. Karataş A, Sonakin Ö, KiliÇarslan M, Baykara T. Poly (Ɛ-caprolactone) microparticles containing levobunolol HCl prepared by a multiple emulsion (w/o/w) solvent evaporation technique: effects of some formulations parameters on microparticle characteristics. J Microencapsul. 2009;26(1):63–74.
8. Karataş A, et al. Ofloxacin loaded electrospun fibers for ocular drug delivery: effect of formulation variables on fiber morphology and drug release. Current Drug Delivery. 2016;13:433–43.
9. Losa C, Marchal-Heussler L, Orallo F, Jato JLV, Alonso MJ. Design of new formulations for topical ocular administration: polymeric nanocapsules containing metipranolol. Pharm Res. 1993;10:80–7.
10. Marchal-Heussler L, et al. Colloidal drug delivery systems for the eye. A comparison of the efficacy of three different polymers: polyisobutylcyanoacrylate polylactic-co-glycolic, acidpolyepsilon-caprolacton. STP Pharma Sci. 1992;2:98–104.
11. Nagarwal RC, Singh PN, Kant S, Maiti P, Pandit JK. Chitosan coated PLA nanoparticles for ophthalmic delivery: characterization, in-vitro and in-vivo study in rabbit eye. J Biomed Nanotechnol. 2010;6:648–57.
12. Salama AH, Abdelkhalek AA, Elkasabgy NA. Etoricoxib-loaded bio-adhesive hybridized polylactic acid-based nanoparticles as an intra-articular injection for the treatment of osteoarthritis. Int J Pharm. 2020;578:119081.
13. Salama AH, Elmotasem H, Salama AA. Nanotechnology based blended chitosan-pectin hybrid for safe and efficient consolidative antiemetic and neuro-protective effect of meclizine hydrochloride in chemotherapy induced emesis. Int J Pharm. 2020;584:119411.
14. Szymanska E, et al. Vaginal chitosan tablets with clotrimazole-design and evaluation of mucoadhesive properties using porcine vaginal mucosa, mucin and gelatine. Chem Pha rm Bull (Tokyo). 2014;62(2):160–7.
15. Niwa T, Takeuchi H, Hino T, Kunou N, Kawashima Y. In vitro drug release behavior of D,L-lactide/glycolide copolymer (PLGA) nanospheres with nafarelin acetate prepared by a novel spontaneous emulsification solvent diffusion method. J Pharm Sci. 1994;83(5):727–32.
16. Alvarez-Alvarez L, et al. Hydrocortisone loaded poly-(3-hydroxybutyrate-co-3-hydroxyvalerate) nanoparticles for topical ophthalmic administration: preparation, characterization and evaluation of ophthalmic toxicity. Int J Pharm. 2019;568:118519.
17. Youssef N, et al. A novel nasal almotriptan loaded solid lipid nanoparticles in mucoadhesive in situ gel formulation for brain targeting: preparation, characterization and in vivo evaluation. Int J Pharm. 2018;548(1):609–24.
18. Basha M, AbouSamra MM, Awad GA, Mansy SS. A potential antibacterial wound dressing of cefadroxil chitosan nanoparticles in situ gel: fabrication, in vitro optimization and in vivo evaluation. Int J Pharm. 2018;544(1):129–40.
19. Souto EB, Mehnert W, Muller RH. Polymorphic behaviour of Compritol888 ATO as bulk lipid and as SLN and NLC. J Microencapsul. 2006;23(4):417–33.
20. Ghadiri M, Fatemi S, Vatanara A, Doroud D, Najafabadi AR, Darabi M, et al. Loading hydrophilic drug in solid lipid media as nanoparticles: statistical modeling of entrapment efficiency and particle size. Int J Pharm. 2012;424(1–2):128–37.
21. Salama AH, Shamma RN. Tri/tetra-block co-polymeric nanocarriers as a potential ocular delivery system of lornoxicam: in-vitro characterization, and in-vivo estimation of corneal permeation. Int J Pharm. 2015;492:28–39.
22. Mittal N, Kaur G. Leucaena leucocephala (Lam.) galactomannan nanoparticles: optimization and characterization for ocular delivery in glaucoma treatment. Int J Biol Macromol. 2019;139:1252–62.
23. Gonzalez-Pizarro R, Silva-Abreu M, Calpena AC, Egea MA, Espina M, García ML. Development of fluorometholone-loaded PLGA nanoparticles for treatment of inflammatory disorders of anterior and posterior segments of the eye. Int J Pharm. 2018;547(1–2):338–46.
24. Yang SC, Lu LF, Cai Y, Zhu JB, Liang BW, Yang CZ. Body distribution in mice of intravenously injected camptothecin solid lipid nanoparticles and targeting effect on brain. J Control Release. 1999;59(3):299–307.
25. Marslin G, Revina AM, Khandelwal VKM, Balakumar K, Sheeba CJ, Franklin G. PEGylated ofloxacin nanoparticles render strong antibacterial activity against many clinically important human pathogens. Colloids Surf B: Biointerfaces. 2015;132:62–70.
26. Rani D, Ahuja M. Carboxymethylation of Lepidium sativum polyuronide, its characterization and evaluation as a nanometric carrier. Int J Biol Macromol. 2017;99:233–40.
27. Ustundag-Okur N, et al. Preparation and in vitro-in vivo evaluation of ofloxacin loaded ophthalmic nano structured lipid carriers modified with chitosan oligosaccharide lactate for the treatment of bacterial keratitis. Eur J Pharm Sci. 2014;63:204–15.
28. Somaia AA, et al. Metabolic profiling of a polyphenolic-rich fraction of *Coccinia grandis* leaves using LC-ESI-MS/MS and in vivo validation of its antimicrobial and wound healing activities. Food Funct. 2019.
29. AbouSamra MM, Salama AH. Enhancement of the topical tolnaftate delivery for the treatment of tinea pedis via provesicular gel systems. J Liposome Res. 2017;27(4):324–34.
30. Hopwood D. Fixatives and fixation: a review. Histochem J. 1969;1(4):323–60.
31. Aldebasi YH, Mohamed HA, Aly SM. Histopathological studies on rabbits infected by bacteria causing infectious keratitis in human through eye inoculation. Int J Health Sci (Qassim). 2014;8(3):257–67.
32. Khalil RM, et al. Preparation and characterization of nystatin loaded solid lipid nanoparticles for topical delivery. Int J Pharm Sci Res. 2013;4:2292–300.
33. Lima FV, Mendes C, Zanetti-Ramos BG, Nandi JK, Cardoso SG, Bernardon JK, et al. Carbamide peroxide nanoparticles for dental whitening application: characterization, stability and in vivo/in situ evaluation. Colloids Surf B: Biointerfaces. 2019;179:326–33.
34. Reich G. In vitro stability of poly(D,L-lactide) and poly(D,L-lactide)/poloxamer nanoparticles in gastrointestinal fluids. Drug Dev Ind Pharm. 1997;23:1191–8.
35. Fontana G, Pitarresi G, Tomarchio V, Carlisi B, San Biagio PL. Preparation, characterization and in vitro antimicrobial activity of ampicillin-loaded polyethylcyanoacrylate nanoparticles. Biomaterials. 1998;19:1009–17.
36. Palacio J, Orozco VH, López BL. Effect of the molecular weight on the physicochemical properties of poly(lactic acid) nanoparticles and on the amount of ovalbumin adsorption. J Braz Chem Soc. 2011;22(12):2304–11.
37. Salama AH, Mahmoud AA, Kamel R. A novel method for preparing surface-modified fluocinolone acetonide loaded PLGA nanoparticles for ocular use: in vitro and in vivo evaluations. AAPS PharmSciTech. 2016;17(5):1159–72.

38. Matloub AA, AbouSamra MM, Salama AH, Rizk MZ, Aly HF, Fouad GI. Cubic liquid crystalline nanoparticles containing a polysaccharide from Ulva fasciata with potent antihyperlipidaemic activity. Saudi Pharm J. 2018;26(2):224–31.
39. Matloub AA, Salama AH, Aglan HA, AbouSamra MM, ElSouda SSM, Ahmed HH. Exploiting bilosomes for delivering bioactive polysaccharide isolated from Enteromorpha intestinalis for hacking hepatocellular carcinoma. Drug Dev Ind Pharm. 2018;44(4):523–34.
40. Mahmoud AA, Salama AH, Shamma RN, Farouk F. Bioavailability enhancement of aripiprazole via silicosan particles: preparation, characterization and in vivo evaluation. AAPS PharmSciTech. 2018;19(8):3751–62.
41. Kumari A, Yadav SK, Pakade YB, Singh B, Yadav SC. Development of biodegradable nanoparticles for delivery of quercetin. Colloids Surf B: Biointerfaces. 2010;80(2):184–92.
42. Ammar HO, Ghorab M, Kamel R, Salama AH. Design and optimization of gastro-retentive microballoons for enhanced bioavailability of cinnarizine. Drug Deliv Transl Res. 2016;6(3):210–24.
43. Ammar HO, Ghorab M, Kamel R, Salama AH. A trial for the design and optimization of pH-sensitive microparticles for intestinal delivery of cinnarizine. Drug Deliv Transl Res. 2016;6(3):195–209.
44. Salama AH, Basha M, El Awdan S. Experimentally designed lyophilized dry emulsion tablets for enhancing the antihyperlipidemic activity of atorvastatin calcium: preparation, in-vitro evaluation and in-vivo assessment. Eur J Pharm Sci. 2018;112:52–62.
45. Kulkarni AR, Soppimath KS, Aminabhavi TM, Rudzinski WE. In-vitro release kinetics of cefadroxil-loaded sodium alginate interpenetrating network beads. Eur J Pharm Biopharm. 2001;51(2):127–33.
46. Kumar S, Himmelstein KJ. Modification of in situ gelling behavior of carbopol solutions by hydroxypropyl methylcellulose. J Pharm Sci. 1995;84:344–8.
47. Kundu PP, Kundu M. Polymer, vol. 42; 2001. p. 2015.
48. Marinal KB, et al. In situ fast gelling formulation of methyl cellulose for in vitro ophthalmic controlled delivery of ketorolac tromethamine. J Appl Polym Sci. 2009;113:241–1246.
49. Kaur IP, Kanwar M. Ocular preparations: the formulation approach. Drug Dev Ind Pharm. 2002;28(5):473–93.
50. Ammar HO, Salama HA, Ghorab M, Mahmoud AA. Nanoemulsion as a potential ophthalmic delivery system for dorzolamide hydrochloride. AAPS PharmSciTech. 2009;10(3):808–19.
51. Singh J, Chhabra G, Pathak K. Development of acetazolamide-loaded, pH-triggered polymeric nanoparticulate in situ gel for sustained ocular delivery: in vitro. Ex vivo evaluation and pharmacodynamic study. Drug Dev Ind Pharm. 2014;40(9):1223–32.
52. Chawla V, Saraf SA. Rheological studies on solid lipid nanoparticle based carbopol gels of aceclofenac. Colloids Surf B: Biointerfaces. 2012;92:293–8.
53. Kanahaiya I, et al. In-situ gel formation for ocular drug delivery system an overview. Asian J Biomed Pharm Sci. 2011;1:1–7.
54. Kaur IP, Garg A, Singla AK, Aggarwal D. Vesicular systems in ocular drug delivery: an overview. Int J Pharm. 2004;269(1):1–14.
55. Sahoo SK, Dilnawaz F, Krishnakumar S. Nanotechnology in ocular drug delivery. Drug Discov Today. 2008;13(3–4):144–51.
56. Bucolo C, Drago F, Salomone S. Ocular drug delivery: a clue from nanotechnology. Front Pharmacol. 2012;3:188.
57. Ameeduzzafar, et al. Formulation and optimization of levofloxacin loaded chitosan nanoparticle for ocular delivery: in-vitro characterization, ocular tolerance and antibacterial activity. Int J Biol Macromol. 2018;108:650–9.
58. Gestri G, Link BA, Neuhauss SC. The visual system of zebrafish and its use to model human ocular diseases. Dev Neurobiol. 2012;72(3):302–27.
59. Jansook P, Ogawa N, Loftsson T. Cyclodextrins: structure, physicochemical properties and pharmaceutical applications. Int J Pharm. 2018;535(1–2):272–84.
60. Hao J, Wang X, Bi Y, Teng Y, Wang J, Li F, et al. Fabrication of a composite system combining solid lipid nanoparticles and thermosensitive hydrogel for challenging ophthalmic drug delivery. Colloids Surf B: Biointerfaces. 2014;114:111–20.